Role of $^{64}CuCl_2$ PET/CT in Detecting and Staging Muscle-Invasive Bladder Cancer: Comparison with Contrast-Enhanced CT and ^{18}F-FDG PET/CT

Arnoldo Piccardo[1], Gianluca Bottoni[1], Cristina Puppo[2], Michela Massollo[1], Martina Ugolini[1], Mehrdad Shoushtari Zadeh Naseri[1], Enrico Melani[2], Laura Tomasello[3], Monica Boitano[4], Andrea DeCensi[4], Beatrice Sambucco[5], Fabio Campodonico[6], Vania Altrinetti[1], Marco Ennas[6], Alessia Urru[7], Carlo Luigi Augusto Negro[8], Luca Timossi[8], Giorgio Treglia[9–11], Carlo Introini*[6], and Francesco Fiz*[1]

[1]*S.C. di Medicina Nucleare, E.O. Ospedali Galliera, Genova, Italy;* [2]*S.C. Radiodiagnostica, E.O. Ospedali Galliera, Genova, Italy;* [3]*U.O. Clinica di Oncologia Medica, IRCCS Ospedale Policlinico San Martino, Genova, Italy;* [4]*S.C. Oncologia Medica, E.O. Ospedali Galliera, Genova, Italy;* [5]*Department of Health Sciences (DISSAL)-Radiology Section, University of Genoa, Genoa, Italy;* [6]*S.C. di Urologia, E.O. Ospedali Galliera, Genova, Italy;* [7]*Diagnostic Imaging Department, Villa Scassi Hospital-ASL 3, Genoa, Italy;* [8]*S.S.A. Urologia dell'Ospedale Evangelico Internazionale, Genova, Italy;* [9]*Faculty of Biomedical Sciences, Università della Svizzera Italiana (USI), Lugano, Switzerland;* [10]*Clinic of Nuclear Medicine, Imaging Institute of Southern Switzerland, Ente Ospedaliero Cantonale, Bellinzona, Switzerland; and* [11]*Department of Nuclear Medicine and Molecular Imaging, Lausanne University Hospital and University of Lausanne, Lausanne, Switzerland*

Molecular imaging of muscle-invasive bladder cancer (MBC) is restricted to its locoregional and distant metastases, since most radiopharmaceuticals have a urinary excretion that limits the visualization of the primary tumor. $^{64}CuCl_2$, a positron-emitting radiotracer with nearly exclusive biliary elimination, could be well suited to exploring urinary tract neoplasms. In this study, we evaluated the feasibility of $^{64}CuCl_2$-based staging of patients with MBC; furthermore, we compared the diagnostic capability of this method with those of the current gold standards, that is, contrast-enhanced CT (ceCT) and ^{18}F-FDG PET/CT. **Methods:** We prospectively enrolled patients referred to our institution for pathology-confirmed MBC staging/restaging between September 2021 and January 2023. All patients underwent ceCT, ^{18}F-FDG, and $^{64}CuCl_2$ PET/CT within 2 wk. Patient-based analysis and lesion-based analysis were performed for all of the potentially affected districts (overall, bladder wall, lymph nodes, skeleton, liver, lung, and pelvic soft tissue). **Results:** Forty-two patients (9 women) were enrolled. Thirty-six (86%) had evidence of disease, with a total of 353 disease sites. On patient-based analysis, ceCT and $^{64}CuCl_2$ PET/CT showed higher sensitivity than ^{18}F-FDG PET/CT in detecting the primary tumor ($P < 0.001$); moreover, $^{64}CuCl_2$ PET/CT was slightly more sensitive than ^{18}F-FDG PET/CT in disclosing soft-tissue lesions ($P < 0.05$). Both PET methods were more specific and accurate than ceCT in classifying nodal lesions ($P < 0.05$). On lesion-based analysis, $^{64}CuCl_2$ PET/CT outperformed ^{18}F-FDG PET/CT and ceCT in detecting disease localizations overall ($P < 0.001$), in the lymph nodes ($P < 0.01$), in the skeleton ($P < 0.001$), and in the soft tissue ($P < 0.05$). **Conclusion:** $^{64}CuCl_2$ PET/CT appears to be a sensitive modality for staging/restaging of MBC and might represent a "one-stop shop" diagnostic method in these scenarios.

Key Words: muscle-invasive bladder cancer; staging; copper; $^{64}CuCl_2$; PET/CT; nuclear medicine

Received Jan. 28, 2024; revision accepted May 13, 2024.

For correspondence or reprints, contact Francesco Fiz (francesco.fiz@galliera.it).

*Contributed equally to this work.

Published online Jul. 25, 2024.

J Nucl Med 2024; 65:1357–1363
DOI: 10.2967/jnumed.124.267474

Bladder cancer represents the seventh most frequent neoplastic disease in adult men (*1*). In about 75% of cases, it is limited to the superficial mucosa and shows a good response to treatment and an excellent prognosis. However, in about one-fourth of patients, it shows a highly aggressive behavior, invading the bladder musculature (*1*). These forms can be associated with nodal and distant metastases, even at the disease onset (*1,2*). In this setting, adequate locoregional and whole-body staging is necessary to decide the most appropriate therapeutic strategy (*1,2*).

CT with contrast enhancement (ceCT) is the standard procedure for staging muscle-invasive bladder cancer (MBC); it is accurate enough to evaluate the local bladder extent as well as meatal or ureteral involvement and to detect distant metastases (*1*). However, given the high rate of relapse after cystectomy—potentially due to occult metastatic disease underestimated by ceCT (*2,3*)—the introduction of a sensitive procedure, ^{18}F-FDG PET/CT, was proposed and finally accepted in recent guidelines, the intention being to better evaluate the lymph node status (*1,2*). In this locoregional setting, ^{18}F-FDG PET/CT can upstage patients in about 20% of cases (*2*). However, the main limitation of ^{18}F-FDG PET/CT is the inability to evaluate the extent of local disease, which is mostly masked by the intense physiologic urinary activity of the bladder and ureters. In this setting, ^{18}F-FDG PET/CT cannot be proposed as a stand-alone imaging procedure but can be proposed as a complementary tool.

$^{64}CuCl_2$ PET/CT has been proposed as an effective imaging procedure for detecting various neoplasms (*4–8*), since copper is highly concentrated in tumors because of its key role in cellular turnover, mitochondrial respiration (*9,10*), carcinogenesis, and cancer metabolism (*11–13*). Copper is required for cytochrome-*c* oxidase activity; limited availability of this element causes tumor cells to switch to less energy-efficient anaerobic glycolysis (*12*). Furthermore, copper

is a key factor in many tumoral pathways, such as superoxide dismutase and BRAF signaling, which control proliferation and neoangiogenesis (*11,14*). Finally, copper is involved in tumor-specific mechanisms that enhance the survivability of the clonal cell (*15*).

Indeed, $^{64}CuCl_2$ PET/CT is a promising tracer for detecting prostate cancer localization and, in particular, for evaluating local relapse after prostatectomy (*6,16*). The advantage of this tracer over others is that its biodistribution is suitable for pelvic molecular imaging, as $^{64}CuCl_2$ is neither excreted nor accumulated in the urinary tract and the bladder. More recently, in 1 pilot study, $^{64}CuCl_2$ PET/CT was proven to detect primary bladder cancer in 5 patients (*17*).

The aims of this study were to evaluate the capability of $^{64}CuCl_2$ PET/CT for staging MBC and to compare the results with those for ceCT and ^{18}F-FDG PET/CT.

MATERIALS AND METHODS

This study was approved by the local ethics committee and by the Agenzia Italiana del Farmaco and the Istituto Superiore di Sanità, which are Italian regulatory agencies of the Ministry of Health. All of the subjects signed a study-specific written informed consent form. The trial was registered in the European Clinical Database (EudractCT no. 2019-002534-37).

Patient Population

From September 2021 to January 2023, we prospectively evaluated all patients affected by histologically confirmed MBC and evaluated at the time of first staging or restaging when metastatic disease was suspected or ascertained. Tumor and nodal staging was based on histopathology; distant metastases were assessed on ceCT and ^{18}F-FDG PET/CT. Table 1 shows the main characteristics of patients and tumors.

Radiopharmaceutical Preparation and PET/CT Acquisition

The Agenzia Italiana del Farmaco approved the manufacture of the experimental $^{64}CuCl_2$ (Sparkle LLC). The radiopharmaceutical was produced as previously described (*4,5,18*): an electroplated ^{64}Ni target was bombarded with a proton current (18 μA;14.6 MeV); the resulting ^{64}Cu was purified using chromatography and an ion-exchange column (Biorad Laboratories). The radioisotope was eluted with concentrated HCl and sieved through a 0.2-μm filter (Millipore; Merck). Radionuclide purity and ^{64}Cu half-life were tested with an HPGe detector (Ortec Ametek) by identifying the characteristic 511-, 1,022-, and 1,345.8-keV photopeaks. A radionuclide purity of greater than or equal to 99.5% was considered acceptable. Radiochemical purity was assessed by reacting [^{64}Cu]$CuCl_2$ with the tetraazacyclotetradecane-*N*,*N*′,*N*″,*N*‴-tetraacetic acid ligand; a purity of greater than or equal to 99% was deemed acceptable. All preparations followed good manufacturing practices.

The tracer was administered intravenously in fasting conditions (>4 h). Whole-body $^{64}CuCl_2$ PET/CT was performed 60 min (*6,19*) after the injection of 370 MBq of $^{64}CuCl_2$. PET scans were acquired in the 3-dimensional mode by a digital PET/CT system (Discovery MI; GE Healthcare). PET/CT scans were acquired via 3-min emissions per bed position from the upper neck to the upper thighs. Raw PET data were reconstructed using an ordered-subset expectation maximization algorithm (2 iterations, 8 subsets, and a 3-mm filter), and the reconstructed voxel size was 2.027 × 2.036 × 2.036 mm; the voxels were arranged in a 256 × 256 matrix.

Low-dose CT was performed for both attenuation correction and topographic localization. ^{18}F-FDG PET/CT was acquired 60 min after tracer injection with the same parameters as in $^{64}CuCl_2$ PET in accordance with European Association of Nuclear Medicine guidelines (*20*). ^{18}F-FDG PET raw data were reconstructed using an ordered-subset expectation maximization algorithm (4 iterations, 8 subsets, and a 5-mm filter); voxel and matrix sizes were the same as in $^{64}CuCl_2$ PET.

TABLE 1
Main Clinical and Histopathologic Features of Patients According to European Association of Urology Guidelines

Feature	Value*
Age (y)	
Median	77
IQR	70–81
Women	9 (21.4)
Histology	
Urothelial epithelium cancer	41 (98)
Adenocarcinoma	1 (2)
T	
T2	26 (62)
T3	5 (12)
T4	11 (26)
N	
N0	3 (7.1)
N1	2 (4.8)
N2	1 (2.4)
N3	1 (2.4)
Nx	35 (83.3)
Tumor location	
Neck or trigone	9 (21)
Walls	33 (79)
NLR	
>3	19 (45)
<3	23 (55)

*Data are reported as numbers of patients, with percentages in parentheses, unless otherwise indicated.

IQR = interquartile range; T = tumor; N = lymph node; NLR = neutrophil-to-lymphocyte ratio.

ceCT

CT scanning was performed using a 64-row multislice CT scanner (Lightspeed VCT; GE Healthcare) and a multiphasic protocol with the administration of contrast material (iopamidol; containing iodine at 370 mg/mL; Bracco). After a basal acquisition, the postcontrast study was performed with a bolus-tracking technique by placing a region of interest in the abdominal aorta at a threshold of 100 Hounsfield units. Three phases were acquired: arterial, venous, and urographic. Arterial phase images were acquired 15 s after enhancement of the thoracic arch (threshold of 100 Hounsfield units), venous phase images were acquired 50 s after the arterial phase, and urographic phase images were acquired 15 min after contrast medium injection. CT parameters were 120 kV, 200–400 mA (using tube current modulation depending on patient size), 0.5-s rotation time, pitch of 1.375:1, and slice thickness of 5 mm. All phases were reconstructed at a slice thickness of 1.25 mm and reformatted in the axial, coronal, and sagittal planes.

Image Interpretation

Two senior nuclear medicine physicians with at least 10 y of experience in PET/CT examinations reviewed all PET images, unaware of other PET/CT and ceCT results. On ^{18}F-FDG PET/CT and $^{64}CuCl_2$ PET/CT, any focal, nonphysiologic uptake higher than the surrounding

TABLE 2
Patient-Based Analysis for Sensitivity, Accuracy, and Specificity

Parameter	Location	ceCT (%)	^{18}F-FDG (%)	$^{64}CuCl_2$ (%)	*P* for ceCT vs. ^{18}F-FDG	*P* for ceCT vs. $^{64}CuCl_2$	*P* for ^{18}F-FDG vs. $^{64}CuCl_2$
Sensitivity	Overall	94	53	97	0.0003	1	0.0002
	Bladder primary tumor	97	13	100	<0.0001	1	<0.0001
	Lymph nodes metastases	93	100	100	1	1	1
	Skeletal metastases	57	100	100	0.248	0.248	1
	Liver metastases	75	50	0	1	0.248	0.479
	Lung metastases	83	83	67	1	1	1
	Soft-tissue metastases	50	42	92	1	0.0736	0.041
Accuracy	Overall	86	52	95	0.0005	0.136	<0.0001
	Bladder primary tumor	98	36	100	<0.0001	1	<0.0001
	Lymph nodes metastases	74	90	95	0.023	0.008	1
	Skeletal metastases	93	98	100	1	1	1
	Liver metastases	98	95	90	1	0.248	0.479
	Lung metastases	95	98	95	1	1	1
	Soft-tissue metastases	83	83	98	1	0.041	0.041
Specificity	Overall	33	50	83	NS	0.248	1
	Bladder primary tumor	100	100	100	1	1	1
	Lymph nodes metastases	64	86	93	0.041	0.013	0.497
	Skeletal metastases	100	97	100	1	1	1
	Liver metastases	100	100	100	1	1	1
	Lung metastases	97	100	100	1	1	1
	Soft-tissue metastases	97	100	100	1	1	1

NS = not significant.

background level was considered pathologic. ^{18}F-FDG PET/CT and $^{64}CuCl_2$ PET/CT studies were interpreted by patient-based analysis and lesion-based analysis. In case of a discrepancy between the 2 examiners, a third expert nuclear medicine physician participated, and the case was resolved by consensus. Tumor-to-background ratios (TBRs) were determined for each lesion on the $^{64}CuCl_2$ and ^{18}F-FDG PET/CT images. The TBR was calculated by dividing the SUV_{max} of the lesion by the SUV_{max} of the pelvic fat (*6*). No SUV_{max} or TBR cutoffs were introduced to assess tumor lesions, although these parameters were calculated to support visual interpretation. All ceCT studies were reviewed by 2 radiologists with at least 10 y of experience and unaware of the results of the PET studies. Primary tumor, perivesical invasion, and adjacent organ involvement were diagnosed when a focal morphologic alteration was detected (*21*). Morphologic criteria were also adopted to distinguish between benign and malignant lymph nodes and to detect distant metastases (*22*). Lymph node metastases were considered when a nodal enlargement (>10 mm in the long axis) was depicted (*23*).

TABLE 3
Lesion-Based Analysis for Sensitivity

Location	ceCT (%)	^{18}F-FDG (%)	$^{64}CuCl_2$ (%)	*P* for ceCT vs. ^{18}F-FDG	*P* for ceCT vs. $^{64}CuCl_2$	*P* for ^{18}F-FDG vs. $^{64}CuCl_2$
Overall	62	70	91	<0.0001	<0.0001	<0.0001
Bladder primary tumor	97	8	100	<0.0001	1	<0.0001
Lymph nodes metastases	43	81	87	<0.0001	<0.0001	0.0077
Skeletal metastases	14	82	98	<0.0001	<0.0001	0.0003
Liver metastases	90	70	0	0.479	<0.0001	<0.0001
Lung metastases	92	81	69	0.133	0.013	0.134
Soft-tissue metastases	70	52	87	0.134	0.136	0.013

Standard of Reference

Histopathology was used as the standard of reference for primary tumor, lymph node, and pelvic soft-tissue (i.e., prostate, seminal vesicle, and ureter) lesions. Additionally, distant metastases underwent a multidisciplinary assessment including clinical and diagnostic follow-up based on ceCT or ^{18}F-FDG PET/CT, performed every 3 mo after enrollment. During the follow-up, ceCT images were evaluated by the radiologist using RECIST criteria (*24*); the aspect of the distant lesions on the images was evaluated in light of the adopted therapeutic strategy to confirm their secondary and pathologic nature. Follow-up procedures were performed for at least 1 y after $^{64}CuCL_2$ PET/CT.

Statistical Methods

Since no literature data on the experimental diagnostic method were used, no formal test hypothesis or sample size calculation was made; therefore, the study was intended as a pilot, and the sample size was determined because of feasibility. Descriptive statistics, including mean, SD, median, and interquartile range, were calculated for continuous data; absolute and relative frequencies were used for categoric factors.

The primary objective was to calculate and compare the sensitivity, specificity, and accuracy of the experimental test (e.g., $^{64}CuCl_2$ PET/CT) with those of the standard tests (ceCT and ^{18}F-FDG PET/CT). This analysis was a patient-based analysis (PBA); sensitivity was reported as a lesion-based analysis (LBA).

The χ^2 and Fisher exact tests were adopted to compare categoric data; the exact McNemar test was used to compare sensitivities, specificities, and accuracies between diagnostic procedures on the same subjects. A 2-tailed, paired test was used to analyze and compare TBRs between scans.

All analyses were done using Stata software (version 17; StataCorp.). Two-tailed probabilities are reported, and a P value of 0.05 was used to define nominal statistical significance.

RESULTS

We prospectively enrolled 42 patients. The main clinical characteristics of these patients are summarized in Table 1. Most of these patients (n° = 31, 74%) were evaluated at the time of first staging, whereas 11 (26%) were included in the case of suspected or determined metastatic disease. Thirty-six of 42 patients showed the primary tumor, locoregional metastases, or distant metastases, and overall, 353 sites of disease were confirmed at our multidisciplinary follow-up. Among these 36 patients, ceCT and $^{64}CuCl_2$ PET/CT proved positive in 34 (94%) and 35 (97%), respectively, and they were significantly more sensitive and accurate ($P < 0.01$) than ^{18}F-FDG PET/CT, which was positive in 19 patients (53%) (Table 2).

On PBA, no significant differences among the 3 diagnostic methods were observed regarding sensitivity, specificity, and accuracy in identifying bone, liver, and lung metastases (Table 2). By contrast, in detecting primary tumors, ceCT and $^{64}CuCl_2$ PET/CT proved significantly more sensitive and accurate than ^{18}F-FDG PET/CT. Indeed, ceCT and $^{64}CuCl_2$ PET/CT identified 30 (97%) and 31 (100%) patients with primary MBC, whereas ^{18}F-FDG PET/CT showed it only in 4 patients (13%).

$^{64}CuCl_2$ PET/CT and ^{18}F-FDG PET/CT proved significantly more specific and accurate in detecting lymph node metastases than ceCT ($P < 0.05$). Moreover, $^{64}CuCl_2$ PET/CT showed slightly higher sensitivity and accuracy in disclosing soft-tissue MBC locations than CeCT and ^{18}F-FDG PET CT (Table 2). Specifically, $^{64}CuCl_2$ PET/CT identified 11 (92%) patients with pelvic soft-tissue disease, whereas ceCT and ^{18}F-FDG/PET could identify only 6 (50%) and 5 (42%), respectively.

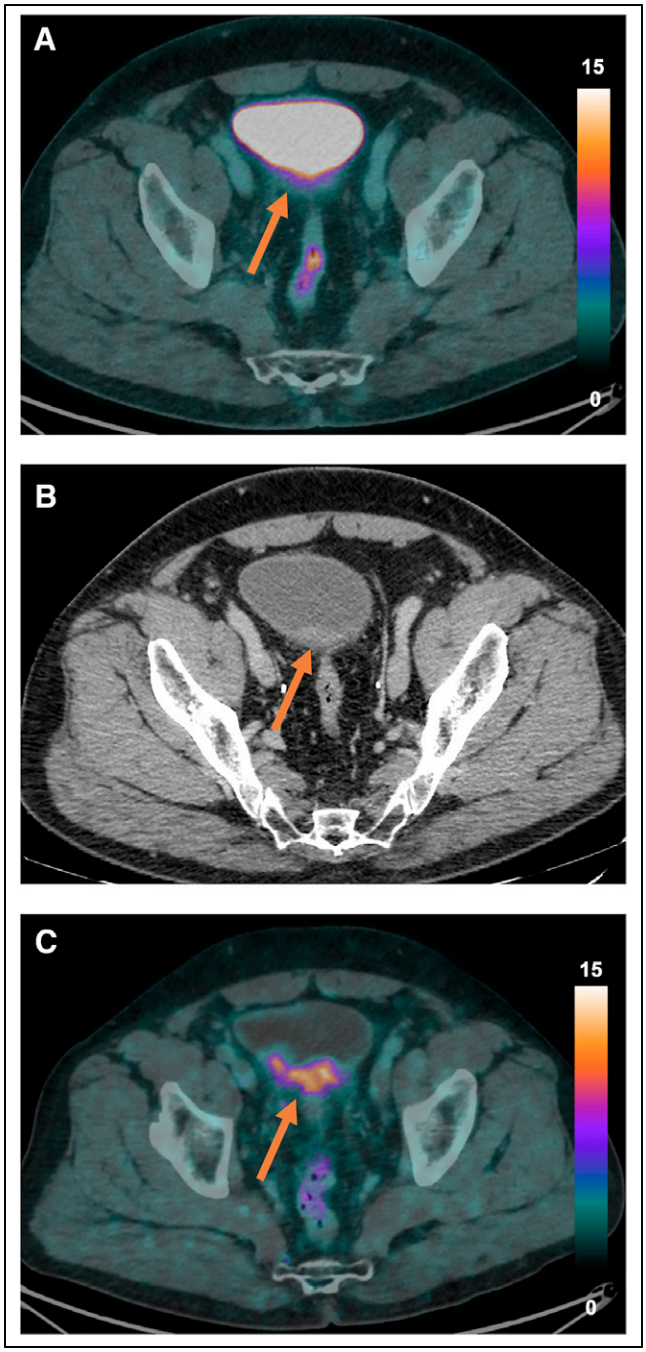

FIGURE 1. Primary tumor. On ^{18}F-FDG PET/CT (A, arrow), urinary activity within bladder hindered visualization of tumor. Conversely, on ceCT (B, arrow), primary tumor was identified as pathologic thickening of posterior bladder wall, showing intense and inhomogeneous $^{64}CuCl_2$ uptake (C, arrow). Uptake intensity is expressed in SUV.

Overall, on LBA, $^{64}CuCl_2$ PET/CT was significantly more sensitive ($P < 0.01$) than the other 2 imaging procedures. Indeed, $^{64}CuCl_2$ PET/CT detected 288 (87%) of the 353 sites of disease, whereas ceCT and ^{18}F-FDG PET/CT showed 191 (54%) and 251 (71%) true positive lesions, respectively (Table 3). When we considered the primary tumor, $^{64}CuCl_2$ PET/CT could detect all primary MBCs and evaluate their extension as accurately as ceCT (Table 3; Fig. 1).

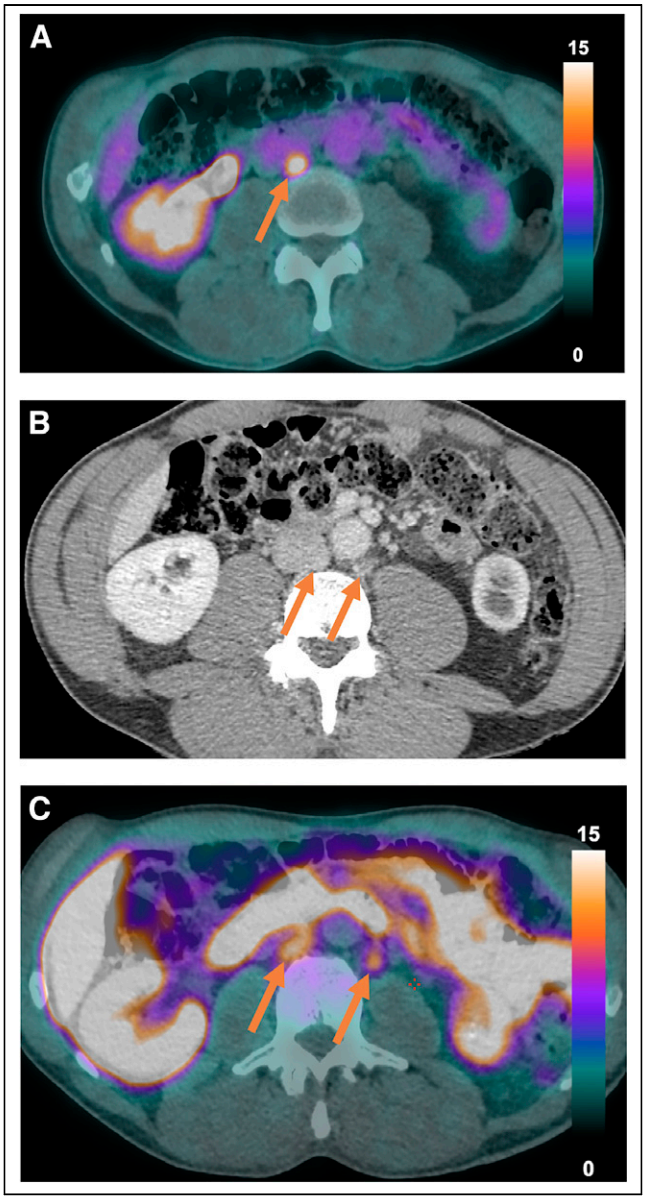

FIGURE 2. Lymph node status on ^{18}F-FDG PET/CT (A), ceCT (B), and $^{64}CuCl_2$ PET/CT (C). Paracaval node showed uptake of both tracers, whereas paraaortic node accumulated $^{64}CuCl_2$ but not ^{18}F-FDG (arrows). Uptake intensity is expressed in SUV.

When we evaluated the different locations of metastatic disease, $^{64}CuCl_2$ PET/CT was significantly more sensitive than ceCT in detecting nodal and bone metastases ($P < 0.01$) (Table 3; Figs. 2–4). Conversely, ceCT was significantly more sensitive than $^{64}CuCl_2$ PET/CT in disclosing lung and liver metastases (Table 3).

$^{64}CuCl_2$ PET/CT was significantly more sensitive than ^{18}F-FDG PET/CT in detecting primary MBC, pelvic soft-tissue localization, and lymph node and bone metastases (Table 3; Figs. 2–4). All ^{18}F-FDG positive metastases showed $^{64}CuCl_2$ uptake, except 4 small lung metastases and the liver metastases.

The mean TBR of ^{18}F-FDG was slightly higher than that of $^{64}CuCl_2$ (9.7 ± 5.2 vs. 7.3 ± 4.9, respectively; $P = 0.0449$). However, in general, the TBRs of the single lesions were not significantly different in the 2 PET methods. In particular, the primary tumor showed TBRs of 6.8 ± 2.6 and 6.3 ± 3.8 in the mean $^{64}CuCl_2$ and ^{18}F-FDG examinations, respectively ($P = 0.571$); similarly, nodal lesions did not show a significantly different uptake (7.4 ± 4.2 vs. 9 ± 4.5, respectively; $P = 0.311$). Skeletal, lung, and soft-tissue lesions also displayed comparable uptake intensities between the 2 methods ($P = 0.964$, 0.335, and 0.061, respectively).

DISCUSSION

This is the first study to evaluate the diagnostic role of $^{64}CuCl_2$ PET/CT in a considerable number of MBC patients prospectively enrolled at the time of first staging or when metastatic disease was suspected or ascertained. Moreover, we compared the $^{64}CuCl_2$ PET/CT results with those of ceCT and ^{18}F-FDG PET/CT, which represent the diagnostic standard procedures according to the recent European Association of Urology guidelines (*1*).

First, all primary MBCs showed high $^{64}CuCl_2$ uptake, corresponding to the wall thickening detected on ceCT. The high expression of human copper transporter (*17,25*), together with the very low activity of the healthy bladder, in which this tracer is not excreted nor accumulated, are the main reasons for the high sensitivity (100%) of $^{64}CuCl_2$ PET/CT in disclosing MBCs. This favorable distributive combination makes $^{64}CuCl_2$ an ideal PET tracer to detect this aggressive tumor and to evaluate its extent (i.e., T stage). From this point of view, $^{64}CuCl_2$ PET/CT could potentially be used as a noninvasive procedure to characterize suspicious wall thickening detected on ceCT or to evaluate disease response after neoadjuvant therapy in confirmed MBC patients. Considering the increasing role of this systemic treatment and the need to evaluate an early response to identifying which patients may benefit from surgery, the use of $^{64}CuCl_2$ PET/CT could avoid delaying radical cystectomy. In our dataset, the $^{64}CuCl_2$ PET method and ceCT seem to be characterized by similar sensitivity, which appears to be higher than what is reported in the literature, where it ranges from 49% to 91% (*26*).

Second, when we investigated the locoregional MBC involvement by analyzing the ability to identify lymph node and pelvic soft-tissue involvement (i.e., seminal vesicles, prostate, and ureteral involvement), we found that both on PBA and LBA, $^{64}CuCl_2$ PET/CT was more accurate than ceCT in detecting lymph node metastases. Furthermore, LBA of $^{64}CuCl_2$ PET/CT proved slightly more sensitive than ceCT in evaluating pelvic soft-tissue infiltration and significantly more sensitive in detecting lymph node metastases. Our data are in keeping with the current literature: CT diagnostic criteria, which use size as a threshold to define the nodal status, might indeed miss a relevant quota of lymph node involvement and are thus characterized by unsatisfying sensitivity, varying between 54% and 86% (*26*).

Additionally, $^{64}CuCl_2$ PET/CT detected significantly more pathologic lymph nodes than ^{18}F-FDG PET/CT. As the diagnostic accuracy of $^{64}CuCl_2$ PET/CT is similar to, or even higher than, that of ceCT and ^{18}F-FDG PET/CT, this new procedure might play a role as a stand-alone imaging tool for detecting locoregional MBC involvement. These findings, if confirmed, can pave the way to using $^{64}CuCl_2$ PET/CT to timely assess patients with borderline renal function or those in whom the MBC has caused acute kidney injury.

Third, when we evaluated the ability to detect distant metastases, we found that only the LBA level of $^{64}CuCl_2$ PET/CT was significantly more sensitive than ceCT and ^{18}F-FDG in disclosing bone metastases. Conversely, $^{64}CuCl_2$ is unsuitable for

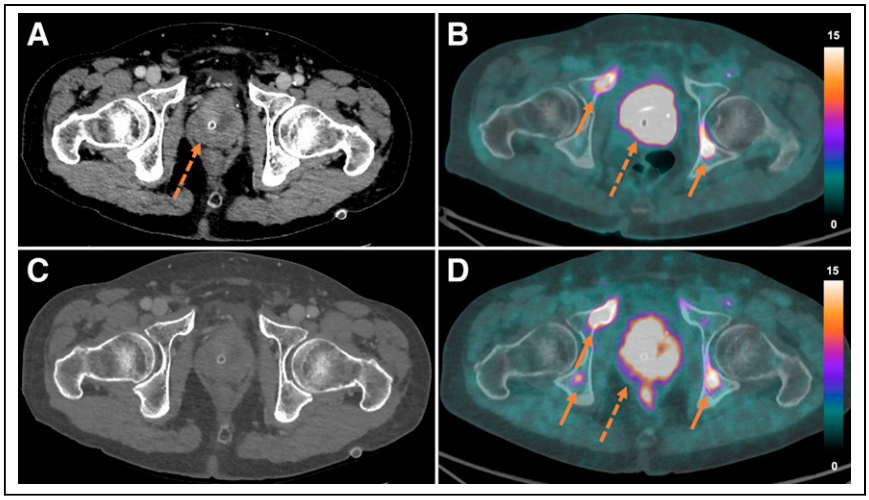

FIGURE 3. Comparison of ceCT (A and C), ^{18}F-FDG PET/CT (B), and $^{64}CuCl_2$ PET/CT (D). On ^{18}F-FDG PET/CT, 2 localizations were seen in pelvic bones (solid arrows); bladder wall (dashed arrow) could not be evaluated because of urinary ^{18}F-FDG activity. On $^{64}CuCl_2$ PET/CT, diffuse uptake in bladder walls was noted (dashed arrow), and additional skeletal localization was disclosed (solid arrows). No bone localization was detected on ceCT. Uptake intensity is expressed in SUV.

investigating liver metastases, given its high physiologic liver concentration. Finally, on LBA, CT proved to be a better method for identifying lung metastases than the 2 PET modalities. However, given the high resolution of the CT component of the hybrid PET/CT imaging, this diagnostic limitation can easily be overcome by performing an additional diagnostic chest CT after the whole-body PET/CT scan.

From the dosimetry point of view, $^{64}CuCl_2$ could imply a higher dose to the patient than ^{18}F-FDG. However, our previous data show a similar dosimetry profile of this tracer compared with established radiopharmaceuticals (*6*). Further development in PET scanner technology should, at any rate, allow a substantial reduction in the administered dose (*27*).

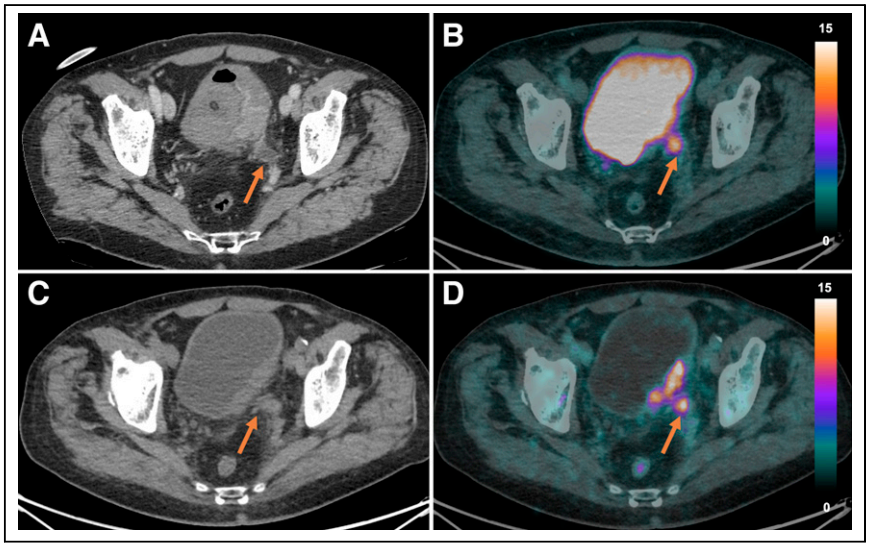

FIGURE 4. Evaluation of disease extension on ^{18}F-FDG PET/CT (B), ceCT (A), and $^{64}CuCl_2$ PET/CT (C and D). Ureter invasion by primary tumor was suspected on ceCT images (A, arrow). On ^{18}F-FDG examination, bladder wall was poorly evaluable; hyperactive spot in distal left ureter appeared as mere dilation (arrow). On $^{64}CuCl_2$ PET/CT, ureteral area was identified as infiltrated by disease (C and D, arrows). Uptake intensity is expressed in SUV.

Despite these encouraging results, some important limitations should be kept in mind. First, the number of MBCs included could have been higher. However, this $^{64}CuCl_2$ cohort represents the largest ever examined since the previous pilot study enrolled only 5 patients (*17*). Additionally, all our patients were prospectively enrolled in a registered clinical trial, and clinical follow-up of at least 1 y was available.

Second, histologic confirmation was not available for all positive lesions. However, 31 of the 42 patients were evaluated at the time of onset, and in all cases, a histologic standard of reference existed. Given that the 11 remaining patients had a suspected or confirmed metastatic disease, we used a multidisciplinary standard of reference based on clinical and diagnostic follow-up, including ceCT or ^{18}F-FDG PET/CT every 3 mo. However, given the absence of a fully independent third evaluation of all metastases (e.g., histopathology), the interpretation of the diagnostic findings could be excessively "imaging-based." The administered activity used for $^{64}CuCl_2$ imaging is higher than that required for ^{18}F-FDG. This parameter was set by the protocol and is also a standard in diagnostic phase-three protocols using the same tracer. Finding the optimal activity for this scenario was beyond the scope of the current investigation; furthermore, the evolution of PET scanners, with the rise of long–axial-field-of-view systems, is likely to reduce the required activity considerably.

Finally, since most patients were enrolled at the first diagnosis, a selection bias might have affected the accuracy of ^{18}F-FDG PET/CT on PBA and LBA, especially concerning the primary tumor and pelvic soft tissue. Indeed, the high ^{18}F-FDG physiologic accumulation in the bladder and urinary tract may have considerably affected the diagnostic performance of this procedure. However, in our analysis, in keeping with the literature (*1,2*), we confirmed the important role of ^{18}F-FDG PET/CT in detecting lymph node metastases missed by ceCT.

CONCLUSION

The biodistribution of $^{64}CuCl_2$ and, in particular, its high uptake in malignancies make $^{64}CuCl_2$ PET/CT a very promising imaging procedure for studying MBC. Its main advantage over the standard imaging procedures is its high accuracy in detecting primary tumor extension, locoregional involvement, and bone metastases; its main limitations are the limited visualization of liver disease and, to a lesser extent, of pulmonary localizations. These results of $^{64}CuCl_2$ PET/CT in MBC, if confirmed by further studies, open the door to possible clinical use of this novel imaging method in this specific oncologic setting.

DISCLOSURE

No potential conflict of interest relevant to this article was reported.

KEY POINTS

QUESTION: Is staging of MBC with $^{64}CuCl_2$ PET/CT feasible, and how does it compare to ceCT and ^{18}F-FDG PET/CT?

PERTINENT FINDINGS: $^{64}CuCl_2$ PET/CT allowed clear visualization of the metabolic activity within the primary tumor. Copper-based PET was more sensitive than ^{18}F-FDG PET/CT in detecting soft-tissue localizations (at both the patient and the lesion levels) as well as nodal and skeletal metastases (at the lesion level).

IMPLICATIONS FOR PATIENT CARE: $^{64}CuCl_2$ PET/CT could be proposed as a "one-stop shop" for MBC staging; in particular, it could have an important role in patients who are not candidates for ceCT, such as those with renal impairment.

REFERENCES

1. Alfred Witjes J, Max Bruins H, Carrión A, et al. European Association of Urology Guidelines on muscle-invasive and metastatic bladder cancer: summary of the 2023 guidelines. *Eur Urol.* 2024;85:17–31.
2. Richters A, van Ginkel N, Meijer RP, et al. Staging fluorodeoxyglucose positron emission tomography/computed tomography for muscle-invasive bladder cancer: a nationwide population-based study. *BJU Int.* 2023;132:420–427.
3. Moschini M, Morlacco A, Briganti A, et al. Clinical lymphadenopathy in urothelial cancer: a transatlantic collaboration on performance of cross-sectional imaging and oncologic outcomes in patients treated with radical cystectomy without neoadjuvant chemotherapy. *Eur Urol Focus.* 2018;4:245–251.
4. Fiz F, Bottoni G, Ugolini M, et al. Diagnostic and dosimetry features of [^{64}Cu]$CuCl_2$ in high-grade paediatric infiltrative gliomas. *Mol Imaging Biol.* 2023;25:391–400.
5. Panichelli P, Villano C, Cistaro A, et al. Imaging of brain tumors with copper-64 chloride: early experience and results. *Cancer Biother Radiopharm.* 2016;31:159–167.
6. Piccardo A, Paparo F, Puntoni M, et al. $^{64}CuCl_2$ PET/CT in prostate cancer relapse. *J Nucl Med.* 2018;59:444–451.
7. Paparo F, Peirano A, Matos J, et al. Diagnostic value of retrospectively fused $^{64}CuCl_2$ PET/MRI in biochemical relapse of prostate cancer: comparison with fused ^{18}F-choline PET/MRI, $^{64}CuCl_2$ PET/CT, ^{18}F-choline PET/CT, and mpMRI. *Abdom Radiol (NY).* 2020;45:3896–3906.
8. Capriotti G, Piccardo A, Giovannelli E, Signore A. Targeting copper in cancer imaging and therapy: a new theragnostic agent. *J Clin Med.* 2022;12:223.
9. Huskisson E, Maggini S, Ruf M. The role of vitamins and minerals in energy metabolism and well-being. *J Int Med Res.* 2007;35:277–289.
10. Horn D, Barrientos A. Mitochondrial copper metabolism and delivery to cytochrome c oxidase. *IUBMB Life.* 2008;60:421–429.
11. Brady DC, Crowe MS, Turski ML, et al. Copper is required for oncogenic BRAF signalling and tumorigenesis. *Nature.* 2014;509:492–496.
12. Ishida S, Andreux P, Poitry-Yamate C, Auwerx J, Hanahan D. Bioavailable copper modulates oxidative phosphorylation and growth of tumors. *Proc Natl Acad Sci USA.* 2013;110:19507–19512.
13. Shanbhag VC, Gudekar N, Jasmer K, Papageorgiou C, Singh K, Petris MJ. Copper metabolism as a unique vulnerability in cancer. *Biochim Biophys Acta Mol Cell Res.* 2021;1868:118893.
14. Juarez JC, Betancourt O Jr, Pirie-Shepherd SR, et al. Copper binding by tetrathiomolybdate attenuates angiogenesis and tumor cell proliferation through the inhibition of superoxide dismutase 1. *Clin Cancer Res.* 2006;12:4974–4982.
15. Tsang T, Posimo JM, Gudiel AA, Cicchini M, Feldser DM, Brady DC. Copper is an essential regulator of the autophagic kinases ULK1/2 to drive lung adenocarcinoma. *Nat Cell Biol.* 2020;22:412–424.
16. Piccardo A, Ugolini M, Righi S, et al. Copper, PET/CT and prostate cancer: a systematic review of the literature. *Q J Nucl Med Mol Imaging.* 2020;64:382–392.
17. Mascia M, Villano C, De Francesco V, Schips L, Marchioni M, Cindolo L. Efficacy and safety of the $^{64}Cu(II)Cl_2$ PET/CT for urological malignancies: phase IIa clinical study. *Clin Nucl Med.* 2021;46:443–448.
18. McCarthy DW, Shefer RE, Klinkowstein RE, et al. Efficient production of high specific activity ^{64}Cu using a biomedical cyclotron. *Nucl Med Biol.* 1997;24:35–43.
19. Righi S, Ugolini M, Bottoni G, et al. Biokinetic and dosimetric aspects of $^{64}CuCl_2$ in human prostate cancer: possible theranostic implications. *EJNMMI Res.* 2018;8:18.
20. Boellaard R, Delgado-Bolton R, Oyen WJG, et al. FDG PET/CT: EANM procedure guidelines for tumour imaging: version 2.0. *Eur J Nucl Med Mol Imaging.* 2015;42:328–354.
21. MacVicar AD. Bladder cancer staging. *BJU Int.* 2000;86(suppl 1):111–122.
22. Kundra V, Silverman PM. Imaging in oncology from the University of Texas M. D. Anderson Cancer Center: imaging in the diagnosis, staging, and follow-up of cancer of the urinary bladder. *AJR.* 2003;180:1045–1054.
23. Vinnicombe SJ, Norman AR, Nicolson V, Husband JE. Normal pelvic lymph nodes: evaluation with CT after bipedal lymphangiography. *Radiology.* 1995;194:349–355.
24. Eisenhauer EA, Therasse P, Bogaerts J, et al. New response evaluation criteria in solid tumours: revised RECIST guideline (version 1.1). *Eur J Cancer.* 2009;45:228–247.
25. Peng F, Lu X, Janisse J, Muzik O, Shields AF. PET of human prostate cancer xenografts in mice with increased uptake of $^{64}CuCl_2$. *J Nucl Med.* 2006;47:1649–1652.
26. Mirmomen SM, Shinagare AB, Williams KE, Silverman SG, Malayeri AA. Preoperative imaging for locoregional staging of bladder cancer. *Abdom Radiol (NY).* 2019;44:3843–3857.
27. Spencer BA, Berg E, Schmall JP, et al. Performance evaluation of the uEXPLORER total-body PET/CT scanner based on NEMA NU 2-2018 with additional tests to characterize PET scanners with a long axial field of view. *J Nucl Med.* 2021;62:861–870.